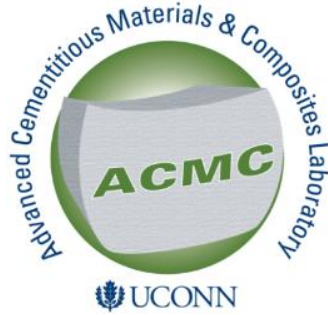


Pyrrhotite Oxidation - Insights into Laboratory Testing of Concrete Expansion and Deterioration, and the Acceleration of Reaction Rates

Sampa Akter (PhD Student)
Meshach Ojo (PhD Student)



Advanced Cementitious Materials & Composites Laboratory
Civil & Environmental Engineering Department
School of Engineering
University of Connecticut
Storrs, CT, USA



ACI Fall 2023 The Concrete Convention and Exposition
American Concrete Institute

Recent Developments in Test Methods and Risk Management for Aggregate Reactions, Part 3 of 3
November 1, 2023, Boston, MA, USA



THE WORLD'S GATHERING PLACE FOR ADVANCING CONCRETE



Outline

- ❑ Part 1: Factors Affecting Iron-sulfide Oxidation in Concrete
- ❑ Conclusion (Part 1)
- ❑ Part 2: Electrochemical Acceleration Method
- ❑ Conclusion (Part 2)

Factors affecting iron-sulfide oxidation in concrete

Table 1: Properties of sulfide bearing aggregates

Aggregate Type	ID	Total Sulfur S_T (%)	Mineralogy (Petrography)	
			main mineral constituents	Iron-sulfide
Connecticut	CT1	1.06	Quartz & Mica	Pyrrhotite
	CT2	0.77		
Canada	CA1	1.18	Plagioclase feldspar, pyroxene, Mica	Pyrrhotite, Pyrite
	CA2	1.25		
Controlled	R	0.04		
Pyrrhotite Rock	Po	25.5		Pyrrhotite
Pyrite	Py	54.1		Pyrite

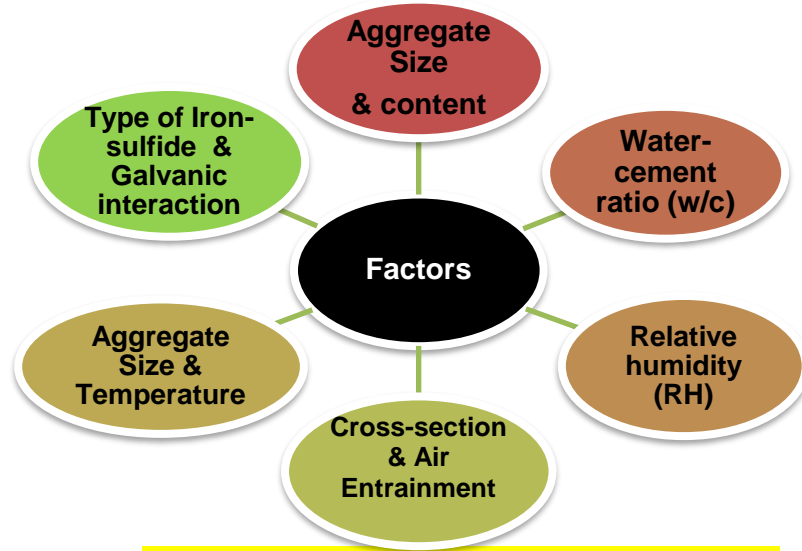
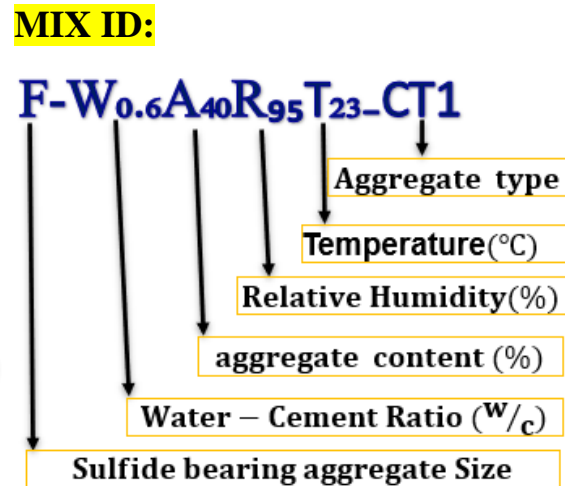


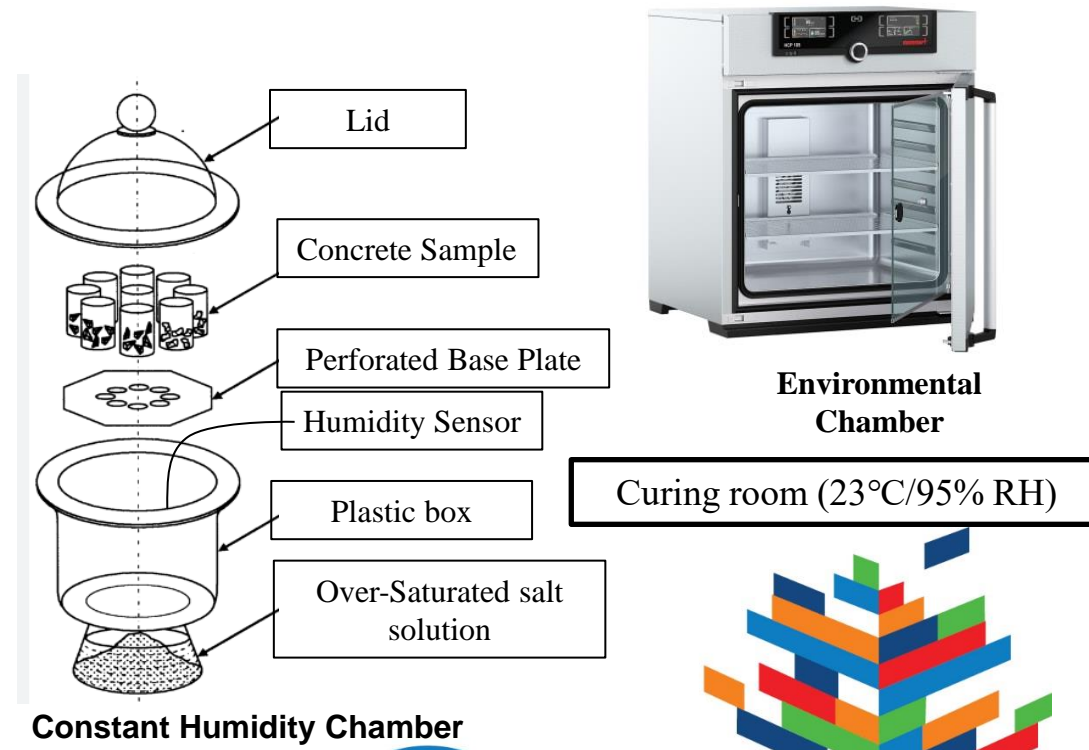
Figure 1: Factors and Testing Condition



Goal

- Determining the factors that speed up iron sulfide oxidation
- Understanding and quantifying deterioration

Constant temperature and humidity Setup



Constant Humidity Chamber

Effect of Sulfur Content and water-cement ratio

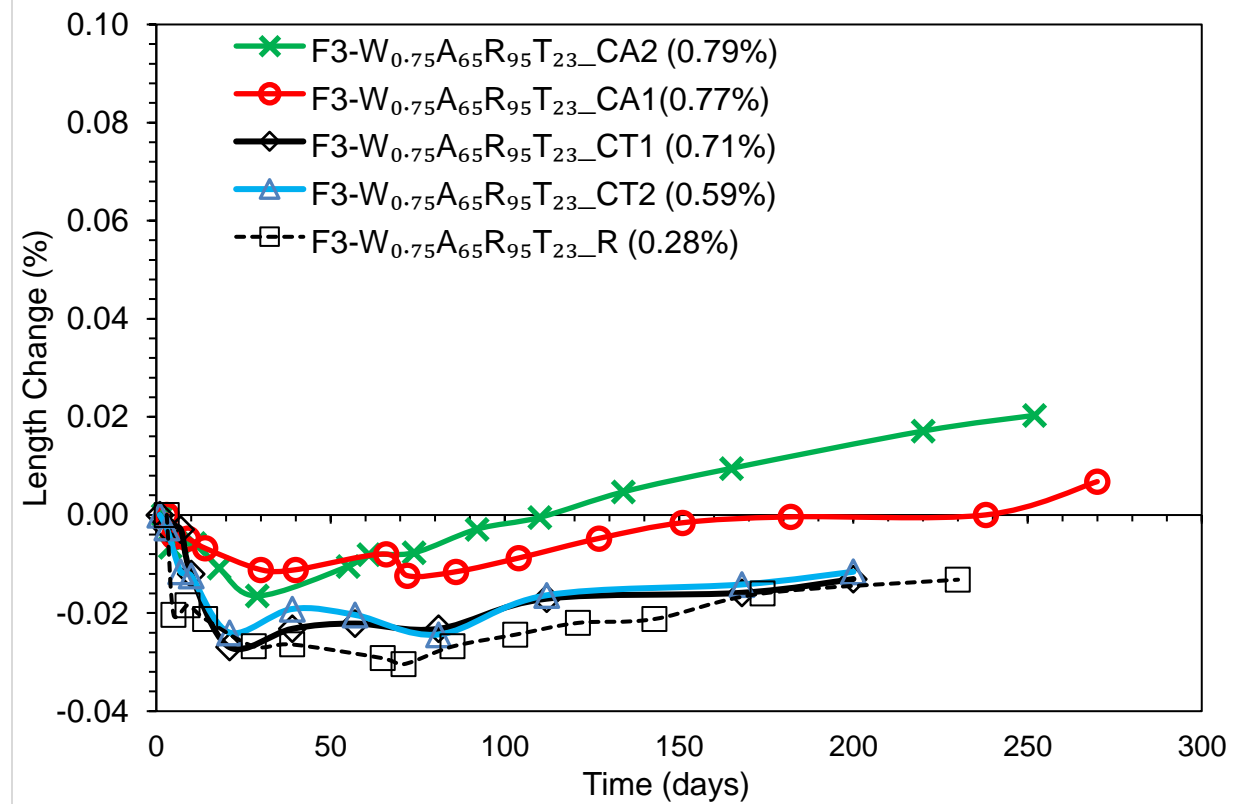
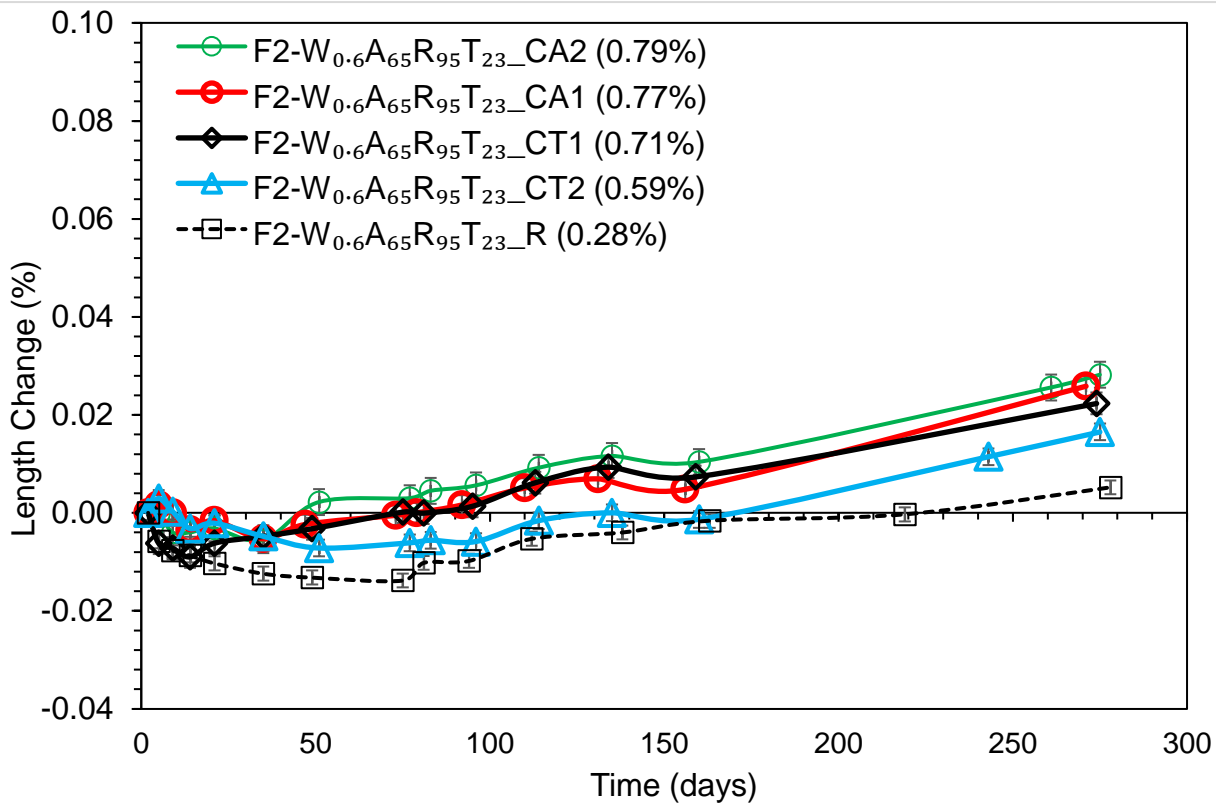


Figure 2: water-cement ratio (w/c) of 0.6

Figure 3: water-cement ratio (w/c) of 0.75



*Each data points corresponds to the AVG of three points

Effect of Relative Humidity (95 and 100%)



Pyrrhotite rock (Po)

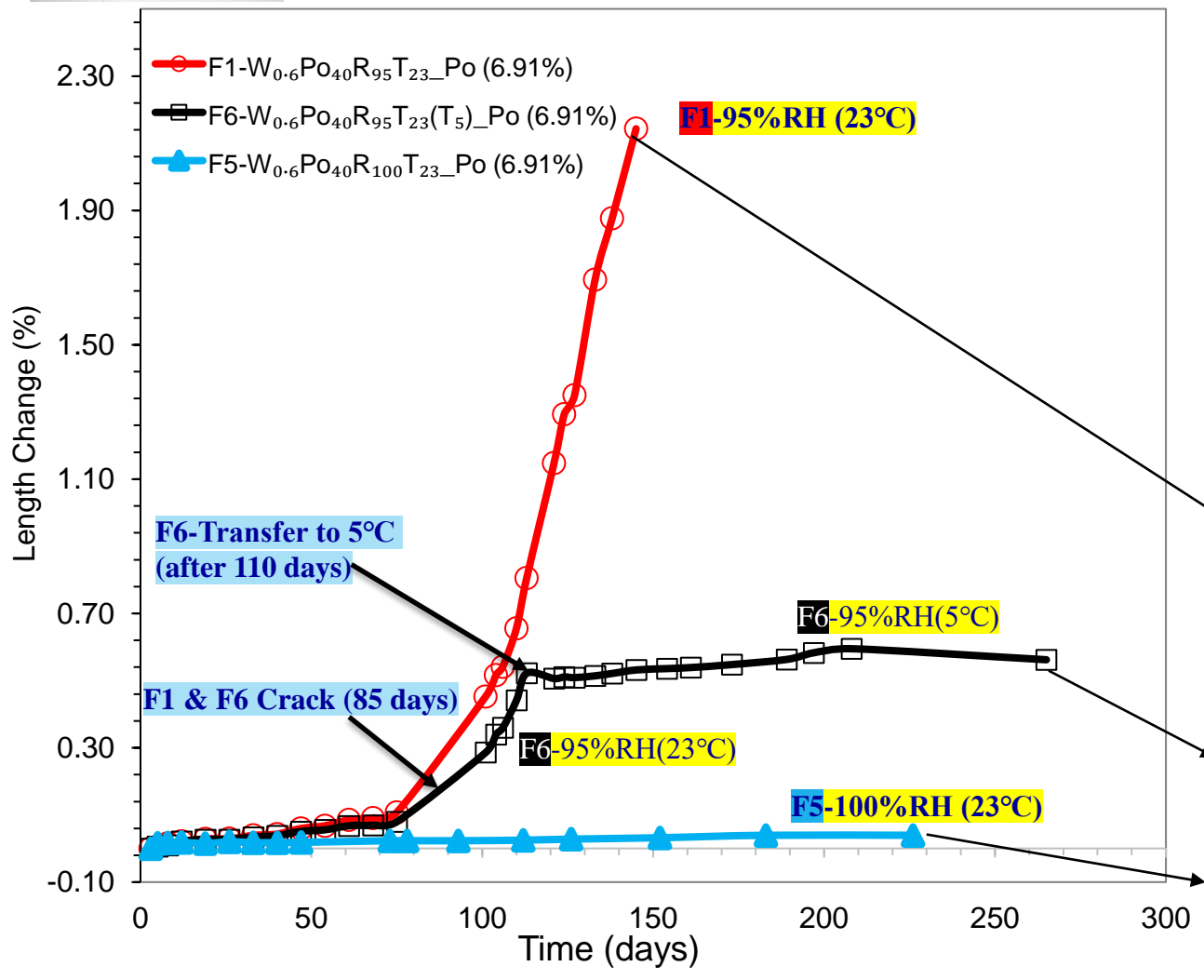


Figure 4: Length change (%) over time

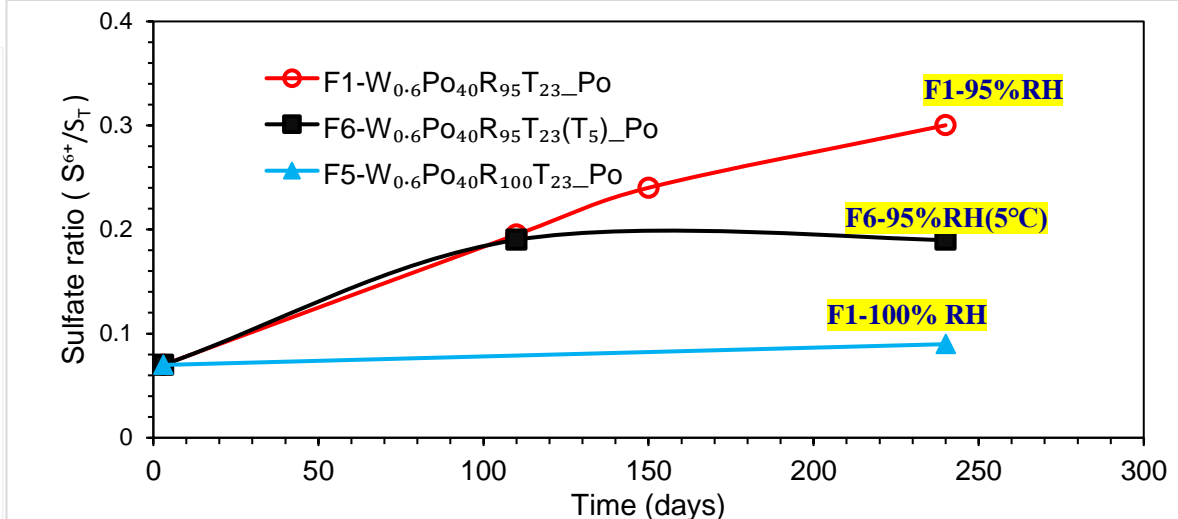
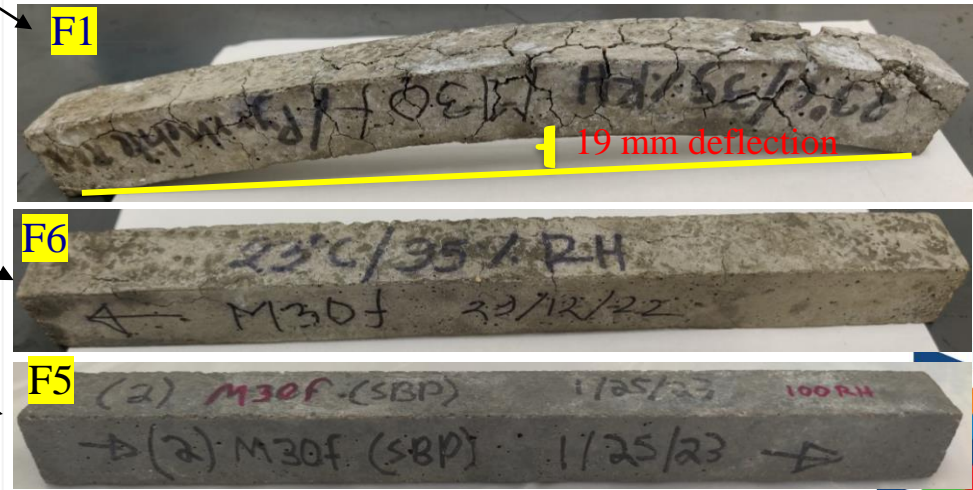


Figure 5: Sulfate generated over time (WD-XRF)





Effect of Relative Humidity (95% and 100%)

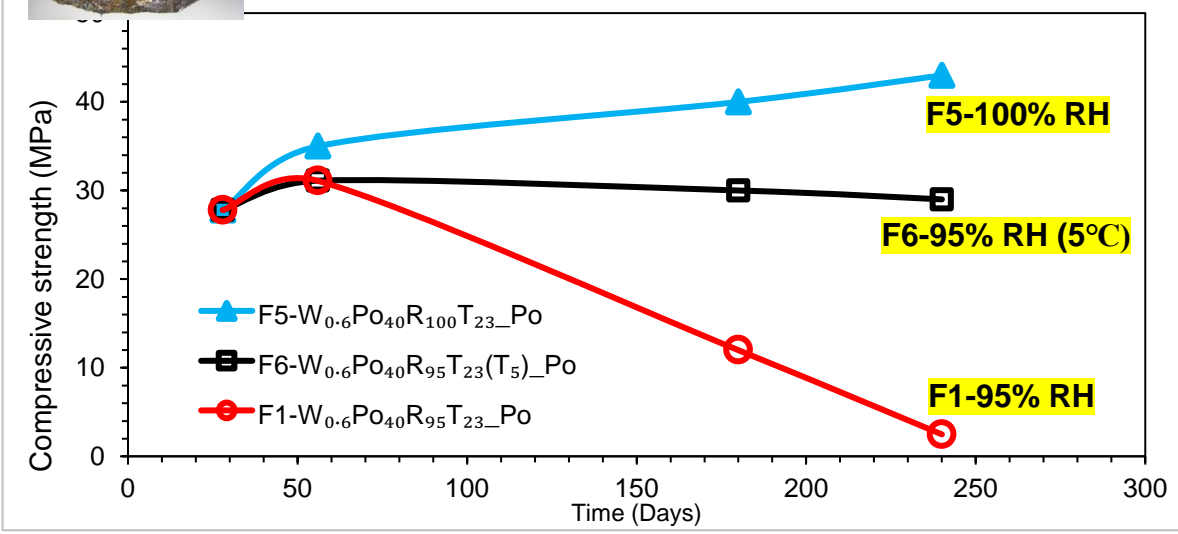


Figure 6: Degradation of concrete compressive strength

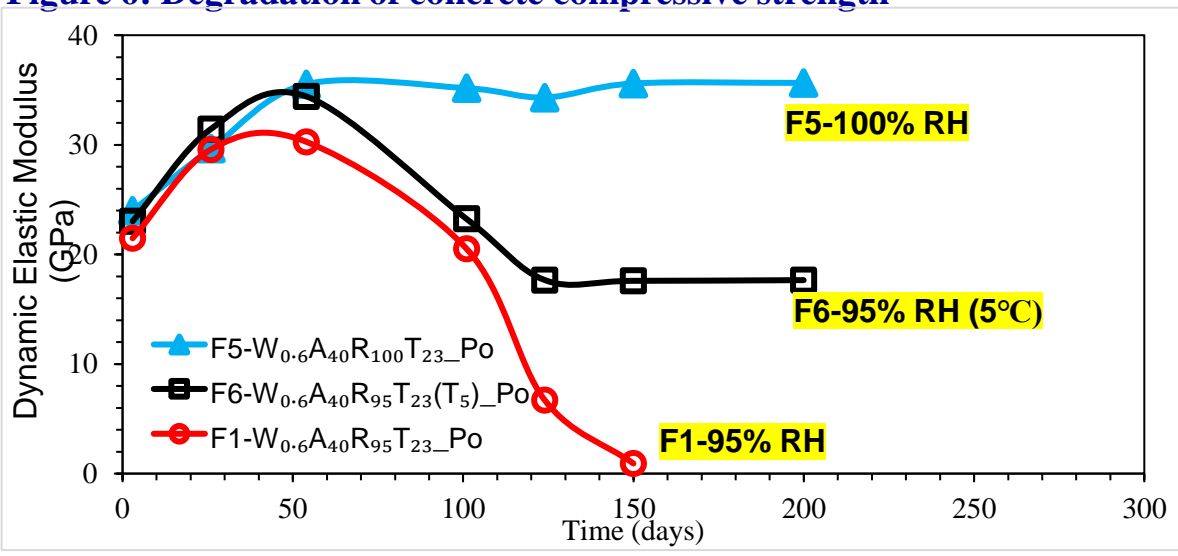
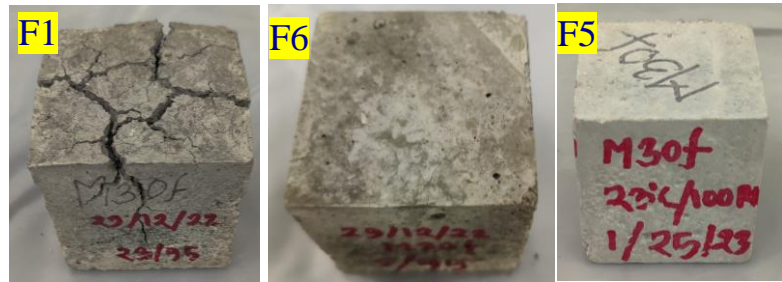


Figure 7: Degradation of Dynamic Elastic Modulus



Concrete cubes specimen at 8 months



Compressive Strength test (ASTM C 109)



Dynamic Elastic Modulus Resonance Frequency Test (ASTM C215)



Pyrrhotite rock (Po)

Effect of concrete cross-section and air-entrainment

25x25 mm

Mortar bar

F1-95%RH



Start cracking **before 3 months** (Age=5 months)

50x50 mm

Cube

F1-95%RH

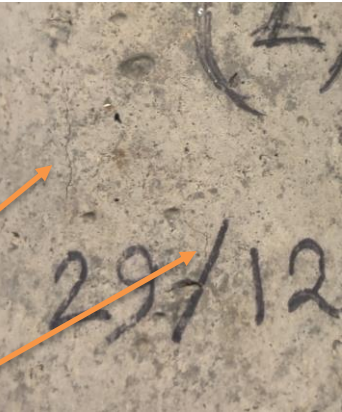


Start cracking **after 3 months** (Age = 8 months)

D (dia)=75 mm

Cylinder

F1-95%RH



Start Cracking **at 10 months** (Age = 10 months)

Figure 8: Effect of concrete cross-section

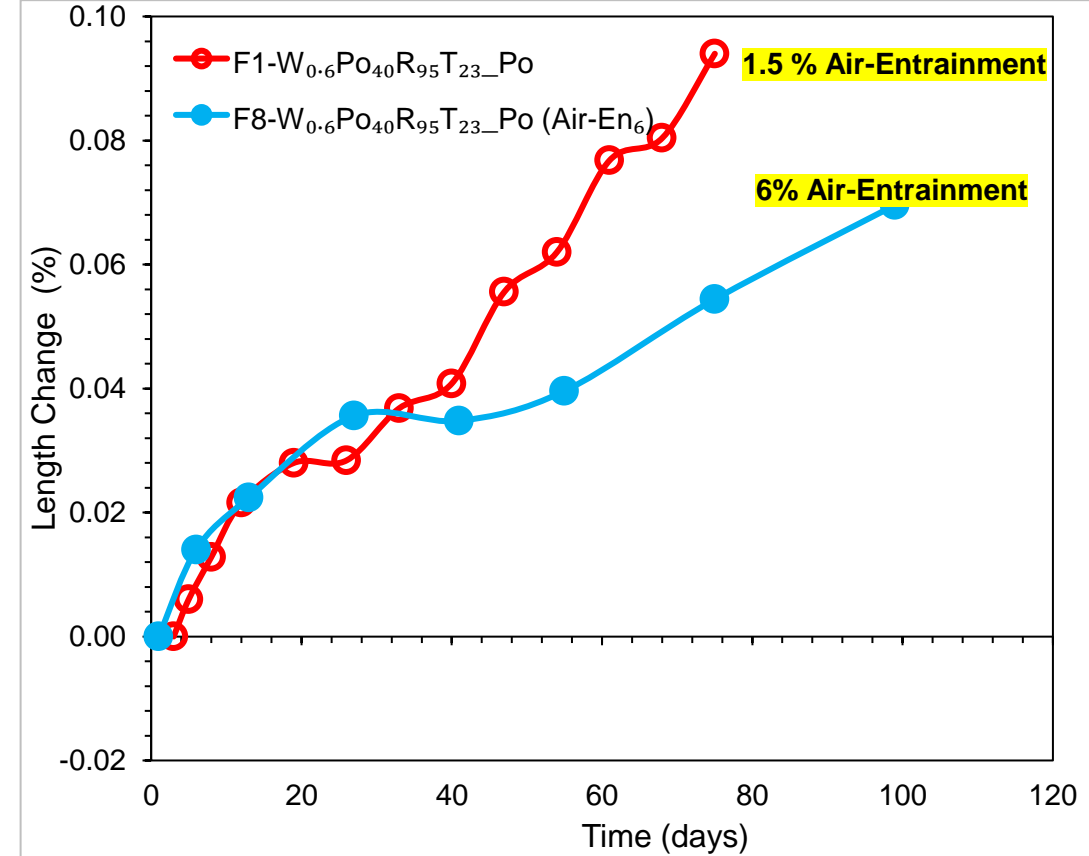


Figure 9: Effect of air-entrainment



Effect of Aggregate Size and Temperature (5 to 80°C)

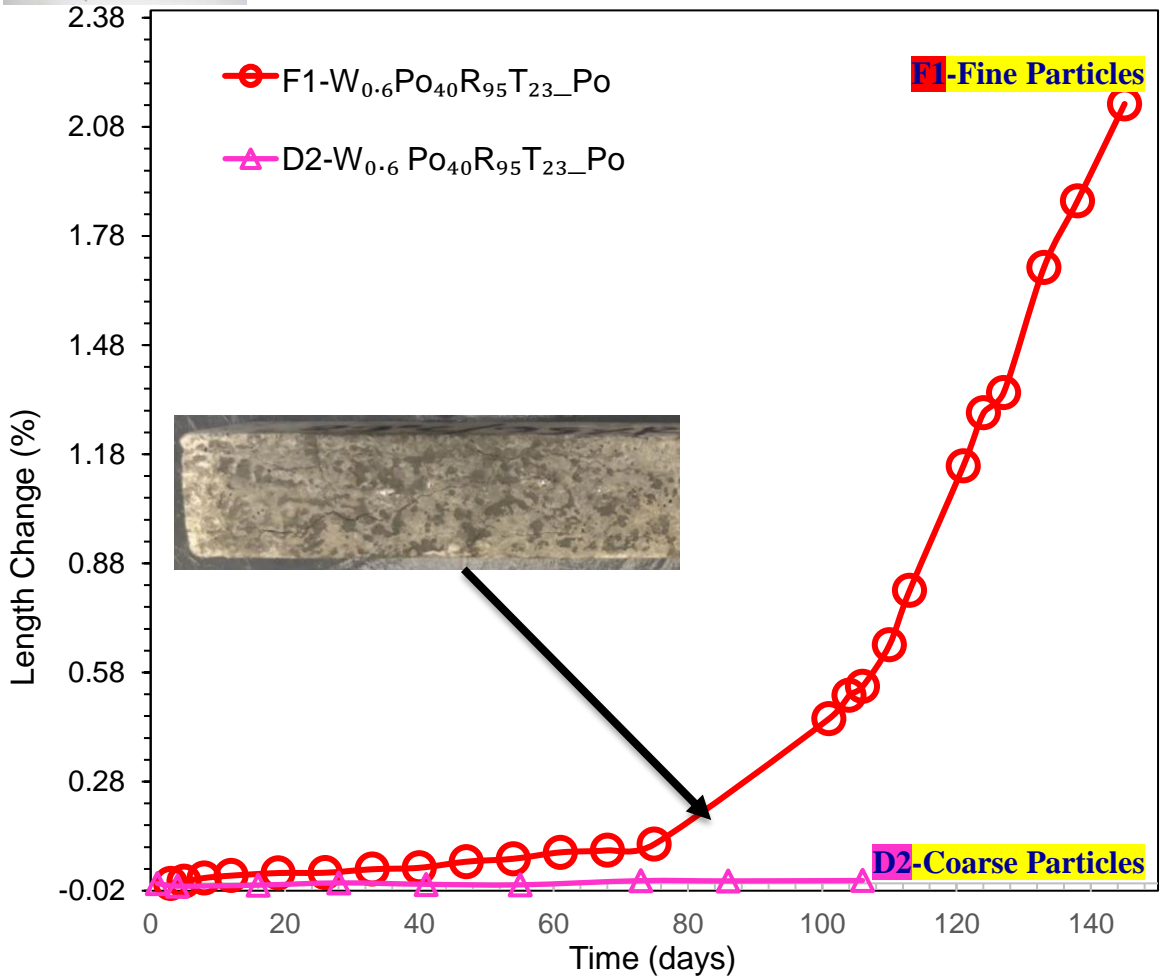


Figure 10: Sulfide bearing aggregate Size

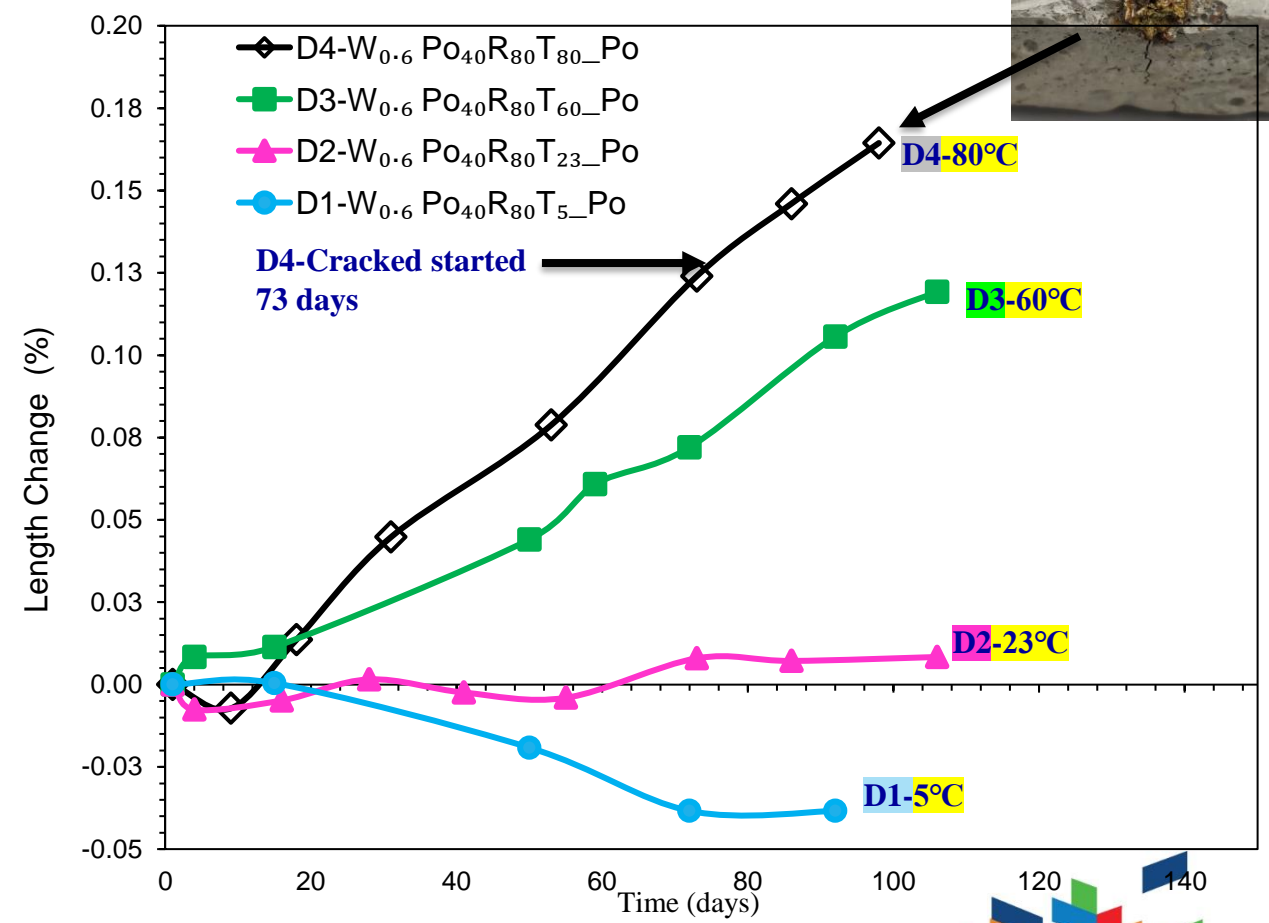


Figure 11: Temperature (5 to 80°C)

Effect of the type of Iron-sulfide and Galvanic interaction



Pyrrhotite rock (Po)



Pyrite (Py)

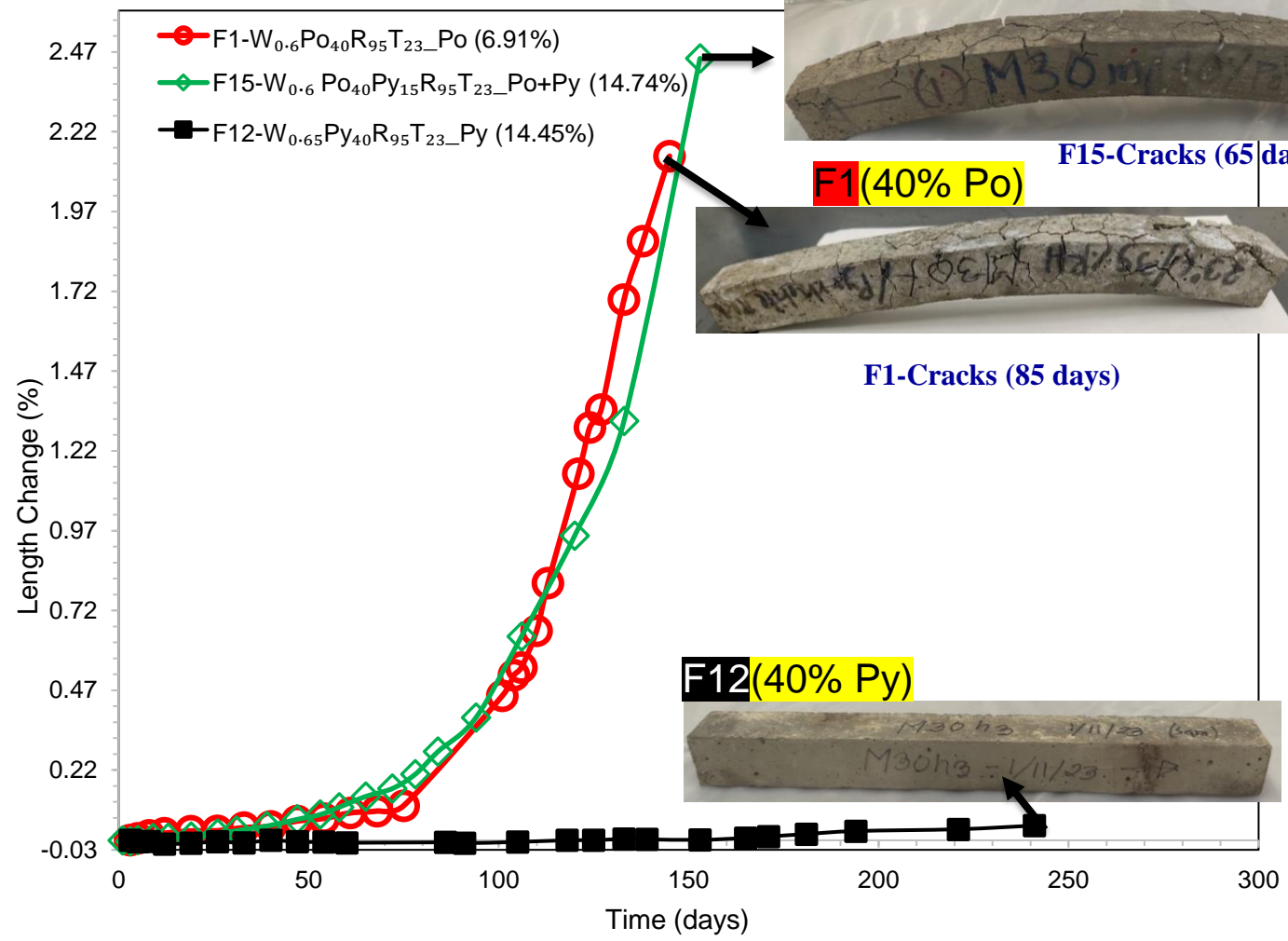


Figure 12: Iron-sulfide type (Pyrrhotite and Pyrite) and galvanic interaction

THE WORLD'S GATHERING PLACE FOR ADVANCING CONCRETE

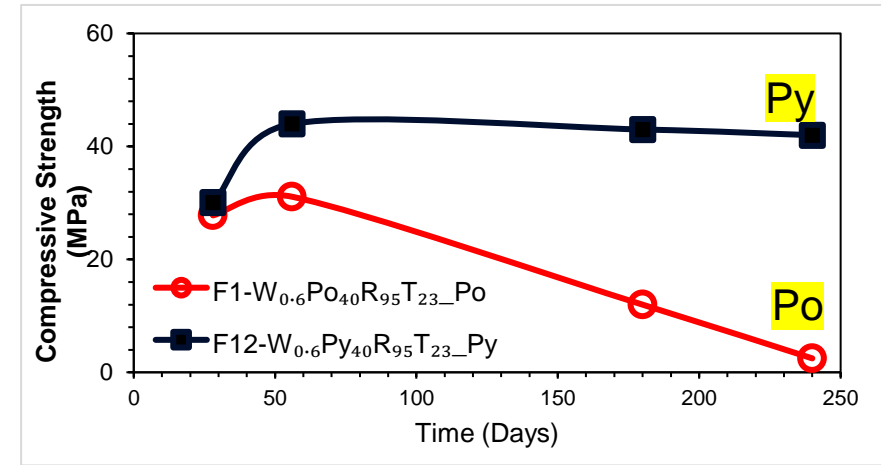


Figure 13: Compressive strength

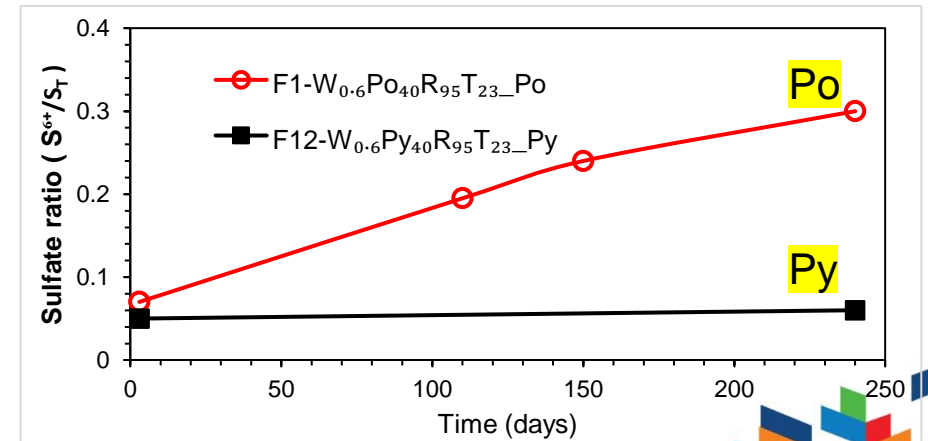


Figure 14: Sulfate generated over time

Effect of the type of iron-sulfide (Pyrrhotite and pyrite)



Conclusion (Part 1)

- ❑ Expansion, concrete compressive strength, dynamic elastic modulus, and sulfate generated over time can be measured to quantify concrete damage caused by iron sulfide oxidation.
- ❑ An excellent correlation exists between expansion, concrete compressive strength, and dynamic elastic modulus including sulfate generation in concrete.
- ❑ Concrete specimens with smaller particle sizes, less air entrainment, and smaller cross-sections exhibited the fastest expansion and cracking due to iron-sulfide oxidation
- ❑ Oxidation rates increase with increasing pyrrhotite content, galvanic interaction, and a temperature of 80°C.
- ❑ A 95% rh showed the greatest expansion in contrast to a 100% rh.
- ❑ Pyrrhotite exhibited almost 100 percent faster oxidation rate than pyrite

Part II: Electrochemical Acceleration Method

- **Overview of Acceleration Method**
- **Accelerated Test Setup Description**
- **Sample Preparation**
- **Results**
- **Conclusion**

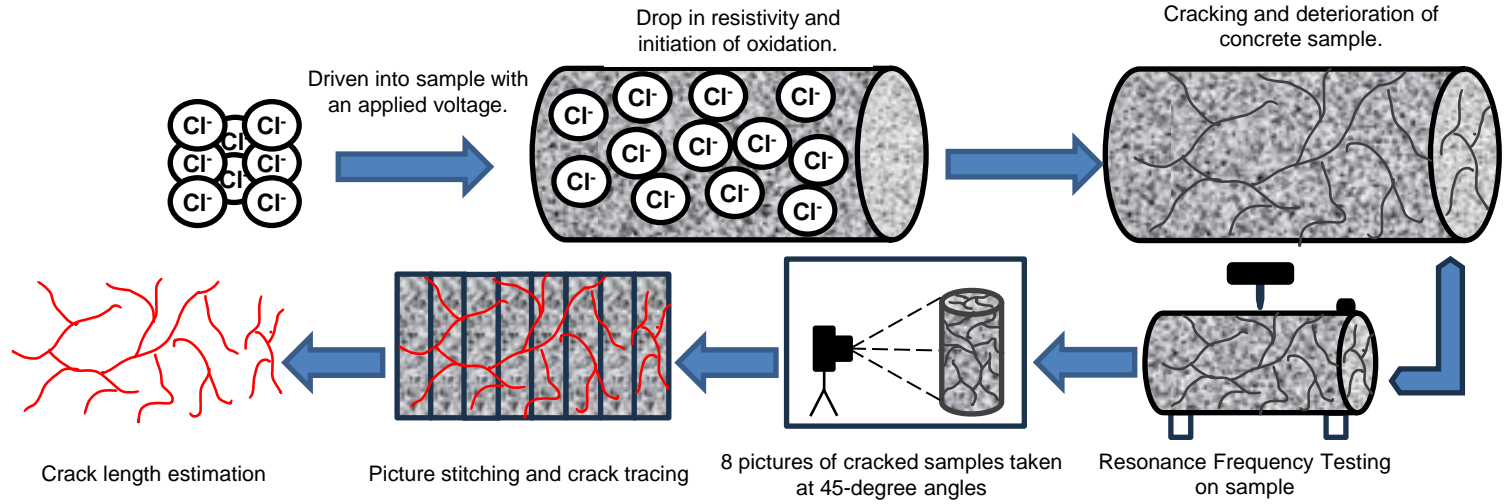
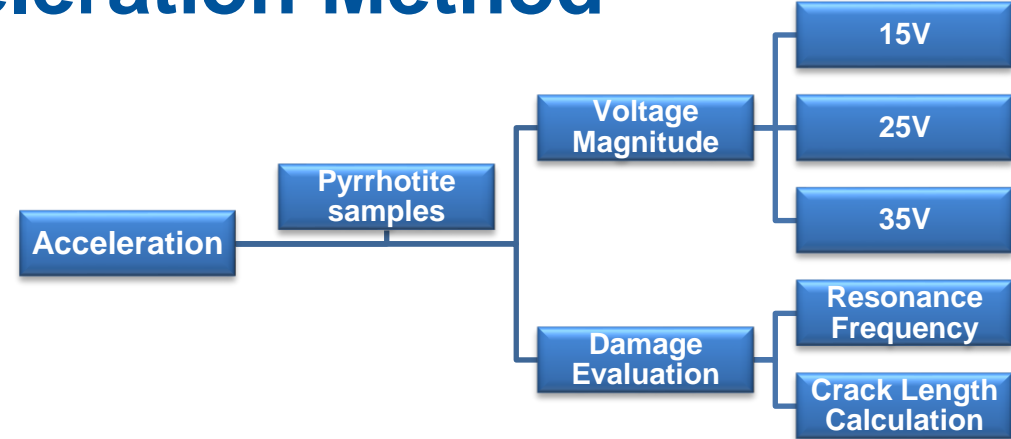
Overview of Acceleration Method

Problems

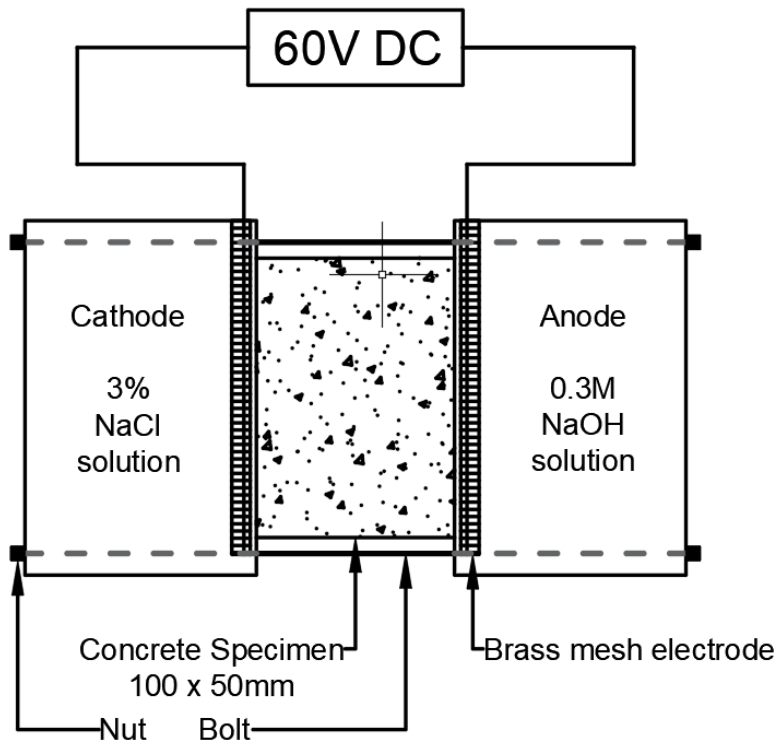
- Interconnected and complicated damage mechanisms.
- Unfeasible timeframe for replicating damage process in a laboratory environment.

Goals

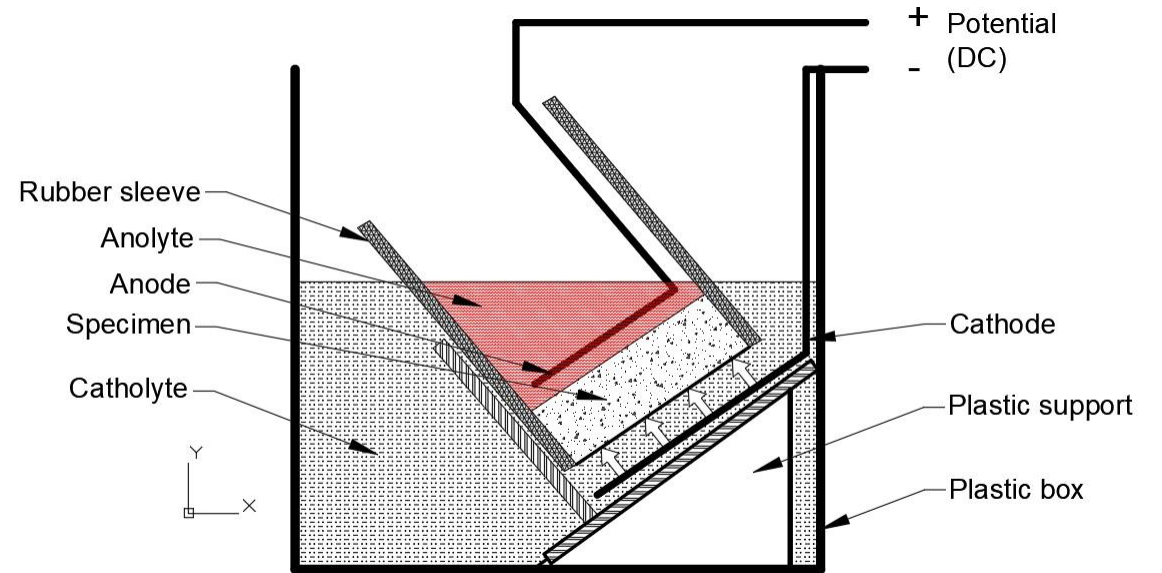
- Identify and define damage parameters.
- Investigate and verify damage parameters of samples in comparison to field deterioration.



Accelerated Test Setup

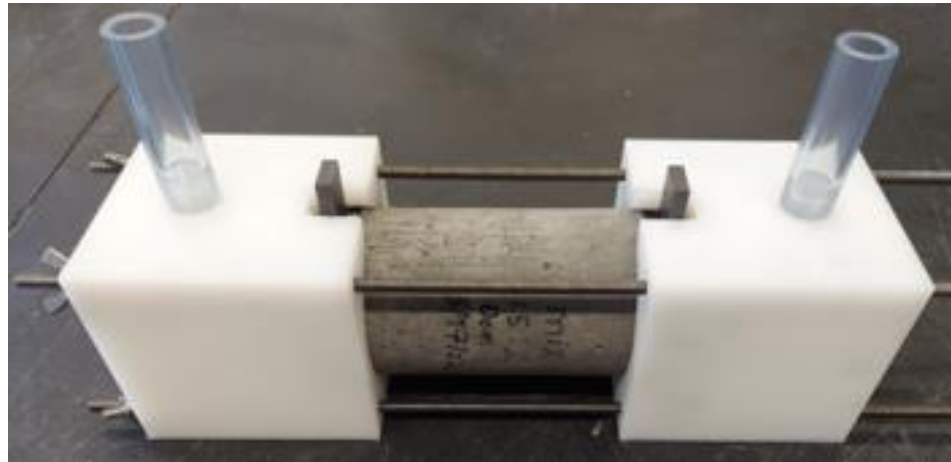
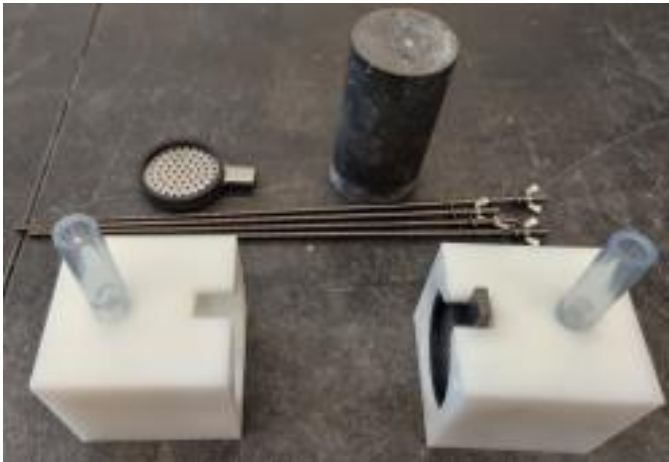
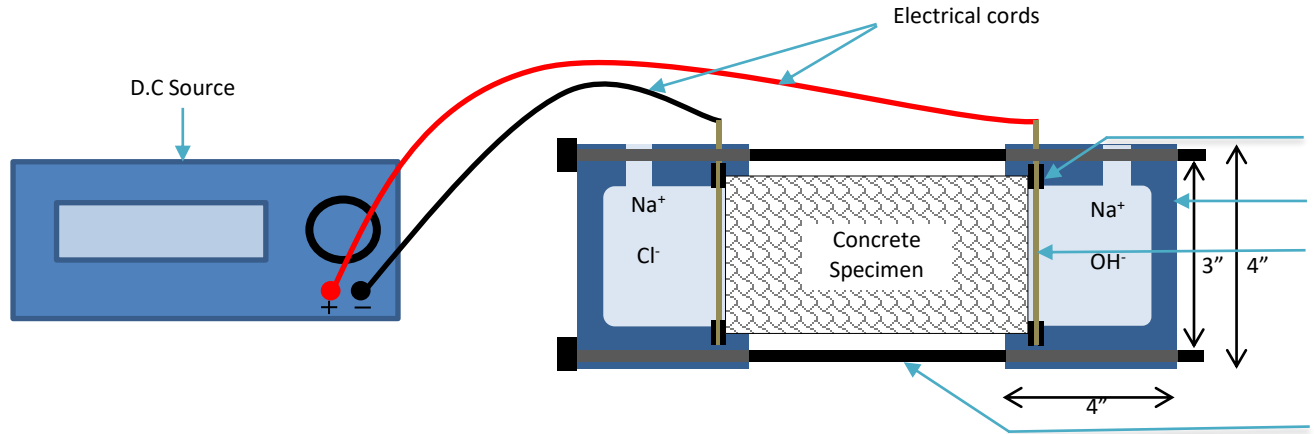


ASTM C1202 – 22 Setup



NT BUILD 492 – 99 Setup

Accelerated Test Setup



Sample Preparation



Pyrrhotite Aggregates (1/2 – 5/8")
Total Sulfur: 1.7%



Control Aggregates (1/2 – 5/8")
Total Sulfur: 0.04%



Casting molds for
(3 x 6)" specimens



Saw-cutting specimen to 4.5"



specimen grinding
for even surface



Ground specimens



Specimens wrapped in plastic
sheets



Specimen in accelerated testing
setup

Accelerated Testing Results (Day 35 at 35V)



Day 84



Pyrrhotite-bearing Sample

Control Sample

Accelerated Testing Results – Field Sample



Field Sample – Day 112



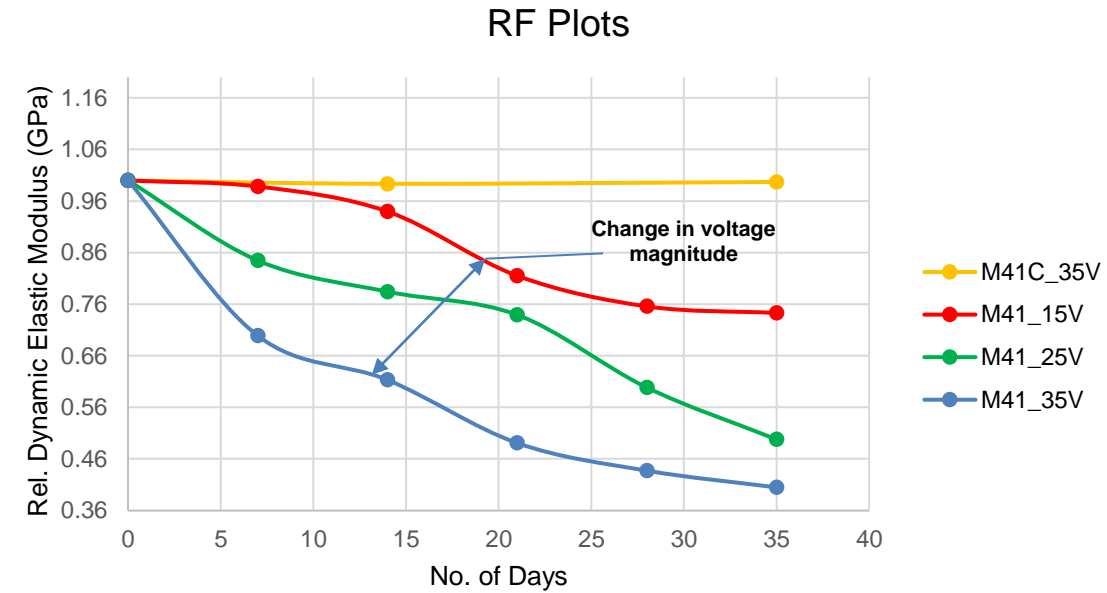
Field Sample – Day 56

Dynamic Elastic Modulus Results from Resonance Frequency



Resonance Frequency Testing

Day	M41_35V			M41_25V			M41_15V			M41C_35V		
	RF (Hz)	E (Gpa)	Rel. E (Gpa)	RF (Hz)	E (Gpa)	Rel. E (Gpa)	RF (Hz)	E (Gpa)	Rel. E (Gpa)	RF (Hz)	E (Gpa)	Rel. E (Gpa)
0	12361	40.21	1.00	12452	40.48	1.00	12347	38.53	1.00	8025	32.24	1.00
14	9681	24.66	0.61	11029	31.76	0.78	11970	36.21	0.94	8026	32.03	0.99
35	7814	16.29	0.41	8721	20.16	0.50	10644	28.63	0.74	8023	32.15	1.00



$$E = CMn^2$$

M = Mass of specimen (kg)

n = Fundamental transverse frequency (Hz)

C = correction factor constant

E = Dynamic elastic modulus



CONCLUSIONS

Employing the adopted electrochemical method effectively accelerated the oxidation and deterioration of laboratory-cast and field concrete samples.

As exposure time to accelerated oxidation increased, RFs and Es in the pyrrhotite-bearing samples and field samples declined, while the control sample remained stable, showing no measurable sign of deterioration.

Higher applied voltages were directly associated with increased oxidation, deterioration rates, and greater reduction in RFs and Es in pyrrhotite-bearing samples.

These findings will aid in understanding the damage evolution, will allow for evaluating the potential risk of concrete failure and will be critical for the study of potential mitigation strategies towards the stability and longevity of residential structures.



Acknowledgments

“This work was performed under the following financial assistance awards 70NANB21H113 & 70NANB23H009 from U.S. Department of Commerce, National Institute of Standards and Technology”

